ELectronics EXpress

REVIEW PAPER

IEICE Electronics Express, Vol.8, No.20, 1642–1662

Digital coherent optical communication systems: fundamentals and future prospects

Kazuro Kikuchi[a)]

Department of Electrical Engineering and Information Systems

The University of Tokyo, 7–3–1 Hongo, Bunkyo-Ku, Tokyo 113–8656, Japan

a) *kikuchi@ginjo.t.u-tokyo.ac.jp*

Abstract: The recently-developed digital coherent receiver enables us to employ a variety of spectrally-efficient modulation formats such as M-ary phase-shift keying (PSK) and quadrature-amplitude modulation (QAM). Moreover, in the digital domain, we can equalize linear transmission impairments, which may stem from group-velocity dispersion (GVD) and polarization-mode dispersion (PMD) of fibers for transmission, because the phase information is preserved after coherent detection.

This paper reviews the history of coherent optical communications, the principle of coherent detection, and the concept of the digital coherent receiver. After that, we discuss digital signal processing (DSP) for mitigating transmission impairments, coherent transmission characteristics of multi-level optical signals, and future prospects of coherent optical communications.

Keywords: coherent optical communications, multi-level modulation, homodyne detection.

Classification: Fiber-optic communication

References

[1] T. Okoshi and K. Kikuchi, *Coherent Optical Communication Systems*, KTK, Tokyo, Kluwer, Dordrecht/Boston/London/Tokyo, 1988.

[2] S. Tsukamoto, D.-S. Ly-Gagnon, K. Katoh, and K. Kikuchi, "Coherent demodulation of 40-Gbit/s polarization-multiplexed QPSK signals with 16-GHz spacing after 200-km transmission," *Proc. Optical Fiber Communication Conference (OFC 2005)*, Anaheim, CA, USA, PDP29, March 2005.

[3] T. Okoshi and K. Kikuchi, "Frequency stabilization of semiconductor lasers for heterodyne-type optical communication systems," *Electron. Lett.*, vol. 16, no. 5, pp. 179–181, Feb. 1980.

[4] Y. Yamamoto, "Receiver performance evaluation of various digital optical modulation-demodulation systems in the 0.5-10 μm wavelength region," *IEEE J. Quantum Electron.*, vol. QE-16, no. 11, pp. 1251–1259, Nov. 1980.

© IEICE 2011

DOI: 10.1587/elex.8.1642

Received August 12, 2011

Accepted August 23, 2011

Published October 25, 2011

[5] R. Griffin and A. Carter, "Optical differential quadrature phase-shift key (oDQPSK) for high capacity optical transmission," *Proc. Optical Fiber Communication Conference (OFC 2002)*, Anaheim, CA, USA, WX6, March 2002.
[6] R. Noé, "Phase noise tolerant synchronous QPSK receiver concept with digital I&Q baseband processing," *Proc. Opto-Electronics and Communications Conference (OECC 2004)*, Yokohama, Japan, 16C2-5, July 2004.
[7] D.-S. Ly-Gagnon, S. Tsukamoto, K. Katoh, and K. Kikuchi, "Coherent detection of optical quadrature phase-shift keying signals with carrier phase estimation," *J. Lightwave Technol.*, vol. 24, no. 1, pp. 12–21, Jan. 2006.
[8] S. Tsukamoto, K. Katoh, and K. Kikuchi, "Coherent demodulation of optical multilevel phase shift-keying signals using homodyne detection and digital signal processing," *IEEE Photon. Technol. Lett.*, vol. 18, no. 10, pp. 1131–1133, May 2006.
[9] Y. Mori, C. Zhang, K. Igarashi, K. Katoh, and K. Kikuchi, "Unrepeated 200-km transmission of 40-Gbit/s 16-QAM signals using digital coherent receiver," *Opt. Express*, vol. 17, no. 32, pp. 1435–1441, Feb. 2009.
[10] M. Taylor, "Coherent detection method using DSP for demodulation of signal and subsequent equalization of propagation impairments," *IEEE Photon. Technol. Lett.*, vol. 16, no. 2, pp. 674–676, Feb. 2004.
[11] S. Tsukamoto, K. Katoh, and K. Kikuchi, "Unrepeated transmission of 20-Gbit/s optical quadrature phase-shift keying signal over 200-km standard single-mode fiber based on digital processing of homodyne-detected signal for group-velocity dispersion compensation," *IEEE Photon. Technol. Lett.*, vol. 18, no. 9, pp. 1016–1018, May 2006.
[12] S. Tsukamoto, Y. Ishikawa, and K. Kikuchi, "Optical homodyne receiver comprising phase and polarization diversities with digital signal processing," *Proc. European Conference on Optical Communication (ECOC 2006)*, Cannes, France, Mo4.2.1, Sept. 2006.
[13] K. Kikuchi and S. Tsukamoto, "Evaluation of sensitivity of the digital coherent receiver," *J. Lightwave Technol.*, vol. 20, no. 13, pp. 1817–1822, July 2008.
[14] S. J. Savory, "Digital filters for coherent optical receivers," *Opt. Express*, vol. 16, no. 2, pp. 804–817, Jan. 2008.
[15] H. Sun, K.-T. Wu, and K. Roberts, "Real-time measurements of a 40-Gb/s coherent system," *Opt. Express*, vol. 16, no. 2, pp. 873–879, Jan. 2008.
[16] L. E. Nelson, S. L. Woodward, M. D. Feuer, X. Zhou, P. D. Magill, S. Foo, D. Hanson, D. McGhan, H. Sun, M. Moyer, and M. O'Sullivan, "Performance of a 46-Gbps dual-polarization QPSK transceiver in a high-PMD fiber transmission experiment," *Proc. Optical Fiber Communication Conference (OFC 2008)*, San Diego, CA, USA, PDP9, Feb. 2008.
[17] M. Birk, P. Gerard, R. Curto, L. E. Nelson, X. Zhou, M. Magill, T. J. Schmidt, C. Malouin, B. Zhang, E. Ibragimov, S. Khatana, M. Glavanovic, R. Lofland, R. Marcoccia, R. Saunders, G. Nicholl, M. Nowell, and F. Forghieri, "Real-time single carrier coherent 100 Gb/s PM-QPSK field trial," *J. Lightwave Technol.*, vol. 29, no. 4, pp. 417–425, Feb. 2011.
[18] K. Kikuchi, "Coherent optical communications: Historical perspectives and future directions," *High Spectral Density Optical Communication Technology*, edited by M. Nakazawa, K. Kikuchi, and T. Miyazaki, Springer Verlag, Heidelberg/Dordrecht/London/New York, Chap. 2, 2010.

© IEICE 2011
DOI: 10.1587/elex.8.1642
Received August 12, 2011
Accepted August 23, 2011
Published October 25, 2011

[19] F. Derr, "Optical QPSK transmission system with novel digital receiver concept," *Electron. Lett.*, vol. 27, no. 23, pp. 2177–2179, Nov. 1991.
[20] C. Zhang, Y. Mori, K. Igarashi, K. Katoh, and K. Kikuchi, "Ultrafast operation of digital coherent receivers using their time-division demultiplexing function," *J. Lightwave Technol.*, vol. 27, no. 3, pp. 224–232, Feb. 2009.
[21] J. K. Fischer, R. Ludwig, L. Molle, C. Schmidt-Langhorst, A. Galperin, T. Richter, C. C. Leonhardt, A. Matiss, and C. Schubert, "High-speed digital coherent receiver with parallel optical sampling," *Proc. Optical Fiber Communication Conference (OFC 2010)*, San Diego, CA, USA, PDPB4, March 2008.
[22] C. Zhang, Y. Mori, K. Igarashi, K. Katoh, and K. Kikuchi, "Ultrafast digital coherent receiver based on parallel processing of decomposed frequency subbands," *Proc. European Conference on Optical Communication (ECOC 2010)*, Torino, Italy, Th.10.A.5, Sept. 2010.
[23] Md. S. Faruk, Y. Mori, C. Zhang, K. Igarashi, and K. Kikuchi, "Multi-impairment monitoring from adaptive finite-impulse-response filters in a digital coherent receiver," *Opt. Express*, vol. 18, no. 26, pp. 26929–26936, Dec. 2010.
[24] S. U. H. Qureshi, "Adaptive equalization," *Proc. IEEE*, vol. 73, no. 9, pp. 1349–1387, Sept. 1985.
[25] D. N. Godard, "Self-recovering equalization and carrier tracking in two-dimensional data communication systems," *IEEE Trans. Commun.*, vol. COM-28, no. 11, pp. 1867–1875, Nov. 1980.
[26] K. Kikuchi, "Performance analyses of polarization demultiplexing based on constant-modulus algorithm in digital coherent optical receivers," *Opt. Express*, vol. 19, no. 10, pp. 9868–9880, May 2011.
[27] Y. Mori and K. Kikuchi, "Carrier-phase-insensitive operation of FIR filters adapted by the decision-directed LMS algorithm in digital coherent optical receivers," *Proc. Opto-Electronics and Communications Conference (OECC 2011)*, Kaohsiung, Taiwan, 7B2-4, July 2011.
[28] K. Kikuchi, "Clock recovering characteristics of adaptive finite-impulse-response filters in digital coherent optical receivers," *Opt. Express*, vol. 19, no. 6, pp. 5611–5619, March 2011.
[29] F. Pancaldi, G. M. Vitetta, R. Kalbasi, N. Al-Dhahir, M. Uysal, and H. Mheidat, "Single-carrier frequency domain equalization," *IEEE Signal Processing Magazine*, pp. 37–56, Sept. 2008.
[30] Md. S. Faruk and K. Kikuchi, "Adaptive frequency-domain equalization in digital coherent receivers," *Opt. Express*, vol. 19, no. 13, pp. 12789–12798, June 2011.
[31] W. Shieh and X. Yi, "High spectral efficiency coherent optical OFDM," in *High Spectral Density Optical Communication Technology*, edited by M. Nakazawa, K. Kikuchi, and T. Miyazaki, Springer Verlag, Heidelberg/Dordrecht/London/New York, Chap. 7, 2010.
[32] K. Kikuchi, "Coherent optical transmission systems," *Proc. Optoelectronics and Communications Conference (OECC 2010)*, Sapporo, Japan, 7B1-1, July 2010.
[33] A. H. Gnauck, P. J. Winzer, S. Chandrasekhar, X. Liu, B. Zhu, and D. W. Peckham, "10×224-Gb/s WDM transmission of 28-Gbaud PDM 16-QAM on a 50-GHz grid transmission over 1,200 km of fiber," *Proc. Optical Fiber Communication Conference (OFC 2010)*, San Diego, CA, U.S.A., PDPB8, March 2010.
[34] A. Sano, T. Kobayashi, K. Ishihara, H. Masuda, S. Yamamoto, K. Mori, E. Yamazaki, E. Yoshida, Y. Miyamoto, T. Yamada, and H. Yamazaki,

© IEICE 2011
DOI: 10.1587/elex.8.1642
Received August 12, 2011
Accepted August 23, 2011
Published October 25, 2011

"240-Gb/s polarization-multiplexed 64-QAM modulation and blind detection using PLC-LN hybrid integrated modulator and digital coherent receiver," *Proc. European Conference on Optical Communication (ECOC 2009)*, Vienna, Austria, PD2.2, Sept. 2009.

[35] M. Nakazawa, S. Okamoto, T. Omiya, K. Kasai, and M. Yoshida, "256 QAM (64 Gbit/s) coherent optical transmission over 160 km with an optical bandwidth of 5.4 GHz," *Proc. Optical Fiber Communication Conference (OFC 2010)*, San Diego, CA, U.S.A., OMJ5, March 2010.

[36] K. Kikuchi, "Analyses of polarization-multiplexed WDM transmission characteristics of high-order optical QAM signals," *Proc. Conference on Lasers and Electro-Optics (CLEO 2011)*, Baltimore, MA, USA, CThH2, May 2011.

[37] K. Kikuchi, "Analyses of wavelength- and polarization-division multiplexed transmission characteristics of optical quadrature-amplitude-modulation signals," *Opt. Express*, vol. 19, no. 19, pp. 17985–17995, Sept. 2011.

[38] K. Kikuchi, "Electronic post-compensation for nonlinear phase fluctuations in a 1000-km 20-Gbit/s optical quadrature phase-shift keying transmission system using the digital coherent receiver," *Opt. Express*, vol. 16, no. 2, pp. 889–896, Jan. 2008.

[39] E. Ip and J. M. Kahn, "Compensation of dispersion and nonlinear impairments using digital backpropagation," *J. Lightwave Technol.*, vol. 26, no. 20, pp. 3416–3425, Oct. 2008.

1 Introduction

Coherent optical fiber communications were studied extensively in the 1980s mainly because of high sensitivity of coherent receivers that could elongate the unrepeated transmission distance [1]; however, since 1990, their research and development had been interrupted behind the rapid progress in high-capacity wavelength-division multiplexed (WDM) systems, which employed the conventional intensity-modulation and direct-detection (IMDD) scheme as well as the erbium-doped fiber amplifier (EDFA) to compensate for span loss of the link.

In 2005, the demonstration of digital carrier-phase estimation in coherent receivers re-stimulated a widespread interest in coherent optical communications [2]. The reason is that the digital coherent receiver enables us to employ a variety of spectrally-efficient modulation formats such as M-ary phase-shift keying (PSK) and quadrature-amplitude modulation (QAM). In addition, since the phase information is preserved after detection, we can equalize linear transmission impairments due to group-velocity dispersion (GVD) and polarization-mode dispersion (PMD) of fibers in the digital domain. These advantages of the born-again coherent receiver have enormous potential for innovating existing optical communication systems. Worldwide efforts are now underway to develop 100-Gbit/s transmission systems based on quadrature PSK (QPSK) modulation, polarization multiplexing, and digital coherent detection at the symbol rate of 25 Gsymbol/s.

This paper reviews the history of coherent optical communications, the

© IEICE 2011
DOI: 10.1587/elex.8.1642
Received August 12, 2011
Accepted August 23, 2011
Published October 25, 2011

principle of coherent detection, and the concept of the newly-developed digital coherent receiver. Next, we discuss digital signal processing (DSP) for mitigating linear transmission impairments, coherent transmission characteristics of multi-level-modulated signals, and future prospects of coherent optical communications. We are going to focus on fundamental aspects of the digital coherent receiver rather than to introduce recently-reported records of coherent transmission systems, which have been smashed every half year.

The organization of the paper is as follows: In Sec.2, we briefly describe the history of coherent optical communications and the impact of the DSP technology. Section 3 deals with the principle of operation of the digital coherent receiver including both of optical circuits and DSP circuits. Section 4 discusses adaptive equalizers, which play the most important role in digital coherent receivers. Algorithms for filter-tap adaptation are also discussed here. Methods of carrier-phase estimation are described in Sec.5. Section 6 discusses coherent transmission characteristics of WDM and polarization-multiplexed (POLMUX) multi-level signals and the influence of fiber nonlinearity on such transmission systems. Section 7 summarizes future prospects of coherent optical communication systems, and finally, in Sec.8, we conclude the paper.

2 Historical background

The research and development of optical fiber communication systems started in the first half of the 1970s. Such systems used intensity modulation of semiconductor lasers, and the intensity of the optical signal transmitted through an optical fiber was directly detected by a photodiode. This combination of the transmitter and the receiver is called the IMDD scheme, which has been commonly employed in optical communication systems up to the present date. The IMDD scheme has a great advantage that the receiver sensitivity is independent of the carrier phase and the state of polarization (SOP) of the incoming signal, which are randomly fluctuating in real systems.

On the other hand, the receiver in which the signal is interfered with a local oscillator (LO) so as to extract the phase information of the signal is called the coherent receiver; heterodyne and homodyne receivers are included in this category. After Okoshi and Kikuchi demonstrated precise frequency stabilization of semiconductor lasers in 1980 [3], aiming at heterodyne detection for optical fiber communications, many demonstrations of coherent optical communication systems were reported until around 1990. With such a coherent receiver, the shot-noise-limited sensitivity can be achieved by injecting a sufficient LO power into the receiver to combat against circuit noise [1, 4]. The motivation of R&D of coherent optical communication systems at this stage was this high receiver sensitivity enabling much longer unrepeated transmission distances.

In the 1990s, however, the development of EDFAs made the shot-noise limited sensitivity of the coherent receiver less significant. This is because the carrier-to-noise ratio (CNR) of the signal transmitted through the ampli-

© IEICE 2011
DOI: 10.1587/elex.8.1642
Received August 12, 2011
Accepted August 23, 2011
Published October 25, 2011

fier chain is determined by the accumulated amplified spontaneous emission (ASE) from EDFAs rather than the shot noise. Technical difficulties in coherent receivers could not be solved by that time. The heterodyne receiver required an intermediate frequency (IF), which should be much higher than the signal bit rate. On the other hand, the homodyne receiver was essentially a baseband receiver; however, the complexity in stable locking of the carrier-phase drift by the optical phase-locked loop (OPLL) prevented its practical applications.

From these reasons, further R&D activities in coherent optical communications had almost been interrupted for nearly twenty years. Meanwhile, the EDFA-based IMDD system started to take benefit from WDM techniques to increase the transmission capacity of a single fiber. The WDM technique thus achieved 1,000 times increase in the transmission capacity during the 1990s.

With such transmission-capacity increase in WDM systems in the 1990s, coherent technologies have restarted to attract a large interest after 2000. The motivation was to cope with the ever-increasing bandwidth demand by coherent technologies. The first step of the revival of coherent optical communications was ignited with optical delay detection of QPSK signals, which is called the DQPSK scheme [5]. In such a scheme, we can double the bit rate, while keeping the symbol rate, and the 40 Gbit/s (20 Gsymbol/s) DQPSK system has now been put into practical use.

The next stage has opened with high-speed digital signal processing (DSP). The recent development of high-speed digital integrated circuits has offered the possibility of retrieving the complex amplitude of the optical carrier from the homodyne-detected signal in a DSP core [6]. The 40-Gbit/s POLMUX QPSK signal was demodulated with a phase-diversity homodyne receiver followed by digital carrier-phase estimation [2, 7], although bit-error rate measurements were done still offline. Since the carrier phase is recovered after homodyne detection by means of DSP, this type of receiver has now been commonly called the "digital coherent receiver." While the optical phase-locked loop (OPLL) technique that locks the LO phase to the signal phase is still difficult to achieve due to the loop-delay problem, DSP circuits are becoming increasingly faster and provide us with simple and efficient means of estimating the carrier phase. Very fast tracking of the carrier phase improves system stability drastically as compared with the OPLL scheme.

Any kind of multi-level modulation format can be introduced by using the coherent receiver [8, 9]. While the spectral efficiency of the binary modulation format is restricted to the Nyquist limit of 1 bit/s/Hz/polarization, multi-level modulation formats can improve this value. The more important advantage of the digital coherent receiver is the post signal-processing function [10, 11]. The demodulation process by the digital coherent receiver is entirely linear; therefore, all of the information on the complex amplitude of the transmitted optical signal is preserved even after detection; and thus, signal processing such as GVD compensation can be performed in the digital domain.

© IEICE 2011
DOI: 10.1587/elex.8.1642
Received August 12, 2011
Accepted August 23, 2011
Published October 25, 2011

The polarization alignment after detection has been made possible by introducing the polarization-diversity scheme into the homodyne receiver [12, 13]. Polarization demultiplexing and compensation for PMD have also been demonstrated with the digital coherent receiver [14], where bulky and slow optical-polarization controllers as well as optical-delay lines are removed.

Since the digital coherent receiver requires high-speed analog-to-digital converter (ADC) and DSP, most of the experiments have been done still offline. However, recently, an application-specific integrated circuit (ASIC) designed for the 11.5-Gsymbol/s POLMUX QPSK signal has been developed [15], and the real-time operation of the digital coherent receiver at the bit rate of 46 Gbit/s has been demonstrated in the field by using such an ASIC [16]. More recently, real-time coherent receivers for 100-Gbit/s POLMUX QPSK signals have been demonstrated by using field-programmable gate arrays (FPGAs) [17]. It is now an urgent task to develop an ASIC for 100-Gbit/s POLMUX QPSK receivers.

3 Principle of operation of the digital coherent receiver

3.1 Coherent optical detection

Figure 1 shows the configuration of the coherent optical receiver called the phase-diversity homodyne receiver or the intradyne receiver [18, 19].

Let the optical signal incoming from the transmitter be

$$E_s(t) = A_s(t)\exp(j\omega_s t), \tag{1}$$

where $A_s(t)$ is the complex amplitude and ω_s the angular frequency. Similarly, the electric field of LO prepared at the receiver can be written as

$$E_{LO}(t) = A_{LO}\exp(j\omega_{LO} t), \tag{2}$$

where A_{LO} is the constant complex amplitude and ω_{LO} the angular frequency of LO. The complex amplitudes A_s and A_{LO} are related to the signal power power P_s and the LO power P_{LO} by $P_s = |A_s|^2/2$ and $P_{LO} = |A_{LO}|^2/2$, respectively.

In the phase-diversity homodyne receiver, $\omega_{LO} \simeq \omega_s$, and the signal phase is not locked to the LO phase. Using the 90° optical hybrid, which gives the 90° phase difference between branched LOs, we can obtain four outputs E_1, E_2, E_3, and E_4 from the two inputs E_s and E_{LO} as

$$E_1 = \frac{1}{2}(E_s + E_{LO}), \tag{3}$$

$$E_2 = \frac{1}{2}(E_s - E_{LO}), \tag{4}$$

$$E_3 = \frac{1}{2}(E_s + jE_{LO}), \tag{5}$$

$$E_4 = \frac{1}{2}(E_s - jE_{LO}). \tag{6}$$

Output photocurrents from balanced photodetectors are then given as

$$I_I(t) = I_1(t) - I_2(t) = R\sqrt{P_s P_{LO}}\cos\{\theta_{sig}(t) - \theta_{LO}(t)\}, \tag{7}$$

© IEICE 2011
DOI: 10.1587/elex.8.1642
Received August 12, 2011
Accepted August 23, 2011
Published October 25, 2011

which is the in-phase component of the signal with respect to the LO phase $\theta_{LO}(t)$, and

$$I_Q(t) = I_3(t) - I_4(t) = R\sqrt{P_s P_{LO}}\sin\{\theta_{sig}(t) - \theta_{LO}(t)\}, \tag{8}$$

which is the quadrature component of the signal. The signal phase is given as $\theta_{sig}(t) = \theta_s(t) + \theta_{sn}(t)$, where $\theta_s(t)$ is the phase modulation and $\theta_{sn}(t)$ the phase noise. Using Eqs. (7) and (8), we can restore the complex amplitude as

$$I(t) = I_I(t) + jI_Q(t) = R\sqrt{P_s(t)\,P_{LO}}\exp\{j(\theta_s(t) + \theta_n(t)\}, \tag{9}$$

where $\theta_n(t)$ is the total phase noise given as

$$\theta_n(t) = \theta_{sn}(t) - \theta_{LO}(t). \tag{10}$$

Equation (9) is equivalent to the complex amplitude of the optical signal except for the phase noise increase by the LO; hereafter, omitting unnecessary constants, we express the restored complex amplitude as

$$E(t) = \sqrt{P_s(t)}\exp\{j(\theta_s(t) + \theta_n(t)\}. \tag{11}$$

In addition, note that such complex amplitude is obtained in the baseband. In order to obtain the phase modulation $\theta_s(t)$, we need to realize the phase-locked condition, $\theta_n(t) = 0$, which means that the LO phase tracks the carrier phase. It is satisfied by using OPLL in the conventional coherent scheme, while it is satisfied by means of DSP in the digital coherent scheme. The DSP-based phase-noise estimation is the heart of the digital coherent receiver.

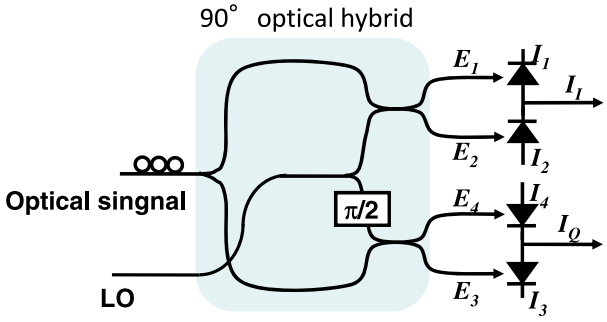


Fig. 1. Configuration of the phase-diversity homodyne receiver using a 90° optical hybrid.

It was assumed up to now that the polarization of the incoming signal was always aligned to that of LO. However, in practical systems, the polarization of the incoming signal is fluctuating. The polarization-diversity receiver can cope with the polarization dependence of the receiver sensitivity. The receiver employing polarization diversity is shown in Fig. 2, where two phase-diversity homodyne receivers are combined in the polarization diversity configuration [12]. The incoming signal having an arbitrary SOP is separated into two linear polarization components with a polarization beam

© IEICE 2011
DOI: 10.1587/elex.8.1642
Received August 12, 2011
Accepted August 23, 2011
Published October 25, 2011

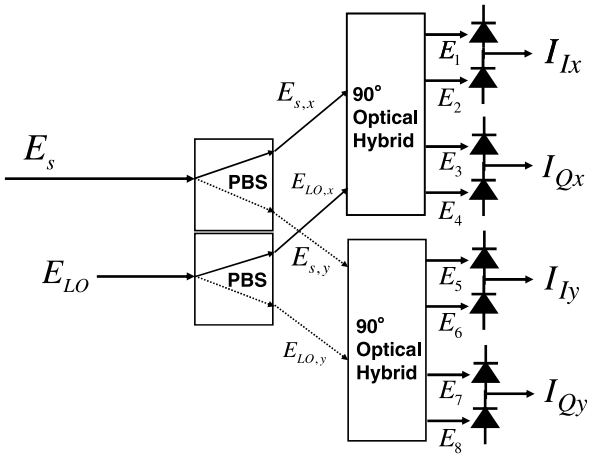


Fig. 2. Configuration of the homodyne receiver employing phase and polarization diversities.

splitter (PBS), which are separately homodyne-detected with LO. We can achieve polarization alignment of the single-polarization signal and demultiplex the dual-polarization signal using this polarization-diversity receiver.

Optical circuits for the coherent receiver comprising phase and polarization diversities have been fabricated by using hybrid integration based on planar lightwave circuits (PLCs) or InP-based monolithic integration.

3.2 DSP circuits

Outputs from the homodyne receiver employing phase and polarization diversities are processed by DSP circuits, and the complex amplitude of the signal is restored in a stable manner despite of fluctuations of the carrier phase and the signal SOP. Symbol-by-symbol control of such time-varying parameters in the digital domain can greatly enhance the system stability compared with optically-controlling methods. In addition, adaptive signal equalization is also a powerful function of DSP.

The DSP circuit is typically composed of the sequence of operations shown in Fig. 3 to retrieve the information from the received signal. First, the four-channel ADC samples the received data and restores the complex amplitude of each polarization. The Nyquist bandwidth of the optical signal with a symbol duration of T is given as $B = 1/T$. Then, outputs from in-phase and quadrature (IQ) ports of the phase-diversity homodyne receiver have the bandwidth of $B/2 = 1/(2T)$, resulting in the Nyquist sampling rate $R = 1/T$ for these signals. When the clock is extracted by an external circuit, we can control the sampling phase for AD converters using the extracted clock; in such a synchronous sampling case, we can employ the Nyquist-rate sampling at $R = 1/T$, which is equal to the symbol rate, because the sampling phase has already been fixed at an optimal value. Then, the signal sampled at the symbol rate is sent to succeeding signal-processing circuits. On the other hand, when the sampling is done asynchronously, we usually need to use $\times 2$ oversampling at $2/T$ to remove the aliasing effect. For example, in 100-Gbit/s POLMUX QPSK systems, the sampling rate is as high as 50 GSample/s,

© IEICE 2011
DOI: 10.1587/elex.8.1642
Received August 12, 2011
Accepted August 23, 2011
Published October 25, 2011

because the symbol rate is 25 Gsymbol/s.

However, drastic increase in the sampling rate of ADC is not easy even by using the state-of-the-art ADC technology. To cope with the difficulty in increasing the sampling rate, a parallelization technique in the time domain has been proposed and demonstrated [20]. In such a scheme, a pulse train is used as an LO light for a digital coherent receiver and samples a part of the waveform under test. Then, multiple receivers, in which delayed pulse trains are used as LO lights, sample the whole waveform in parallel. When the enhanced sampling rate of the interleaved pulse train meets the Nyquist sampling rate, we can reconstruct the waveform with the serialization process in the digital domain [21]. On the other hand, [22] has proposed and demonstrated an alternative approach based on parallel signal-processing in the frequency domain. The receiver detects frequency subbands of an optical signal in parallel by using an optical frequency comb as an LO light. Since each subband has a bandwidth and a Nyquist sampling rate smaller than those of the original signal, low-speed electronics can process the subband information and reconstruct the original signal.

Let E_x and E_y be complex amplitudes in the digital domain, which are obtained from the x-polarization port and the y-polarization port, respectively. These are filtered out to select a desired WDM channel and equalized by an fixed equalizer, which removes inter-symbol interference (ISI) stemming from fixed GVD of the link. Next, the dual-polarization signal is demultiplexed and PMD is compensated for with an adaptive equalizer. When the sampling is done asynchronously, clock recovery can also be achieved at the adaptive equalization stage. Then, the carrier phase is estimated, and the symbol is decoded.

In the following sections, we are going to discuss more details of the DSP circuits.

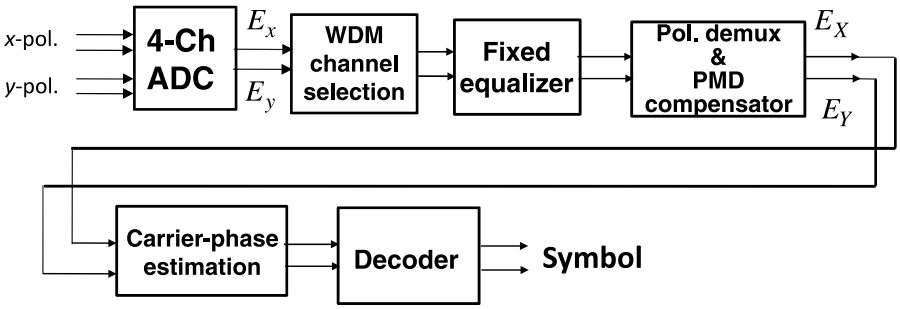


Fig. 3. Typical sequence of digital signal processing for decoding the symbol.

4 Adaptive equalization

4.1 Adaptive FIR filter

If the input power launched on a transmission link is low enough to operate in the linear region, the transfer function of the link can be modeled as a con-

© IEICE 2011
DOI: 10.1587/elex.8.1642
Received August 12, 2011
Accepted August 23, 2011
Published October 25, 2011

catenation of the scalar GVD element $D(\omega)$, the two-by-two unitary matrix for PMD $\mathbf{U}(\omega)$, the two-by-two Hermite matrix for polarization-dependent loss (PDL) $\mathbf{T}$, and the unitary Jones matrix expressing the birefringence $\mathbf{K}$ [23]:

$$\mathbf{H}(\omega) = D(\omega)\mathbf{U}(\omega)\mathbf{TK}, \tag{12}$$

where ω is the angular frequency of the optical carrier. The transfer matrix of the equalizer in the digital coherent receiver $\mathbf{H}_{eq}(\omega)$ should be the inverse matrix of $\mathbf{H}(\omega)$ as

$$\begin{aligned} \mathbf{H}_{eq}(\omega) &\simeq \mathbf{H}(\omega)^{-1} \\ &= \begin{bmatrix} h_{xx}(\omega) & h_{xy}(\omega) \\ h_{yx}(\omega) & h_{yy}(\omega) \end{bmatrix}. \end{aligned} \tag{13}$$

The input vector for the n-th sampled signal is expressed as $[E_x(n), E_y(n)]^{\mathrm{T}}$. On the other hand, the output vector is written as $[E_X(n), E_Y(n)]^{\mathrm{T}}$. Each element of the matrix $h_p(\omega)$ $(p = (xx, xy, yx, yy))$ can be realized by a finite-impulse-response (FIR) filter; then, the matrix given by Eq. (13) is implemented in two-by-two butterfly-structured FIR filters shown in Fig. 4 [14]. Let the number of taps of FIR filters be k, and the delay-time interval be given as T/m, where T denotes the symbol interval and m is an integer showing the oversampling ratio of AD conversion. Input column vectors $\overrightarrow{E_x}(n)$ and $\overrightarrow{E_y}(n)$ for the FIR filter are defined as

$$\overrightarrow{E_x}(n) = [E_x(n), E_x(n-1), \cdots, E_x(n-k-2), E_x(n-k-1)]^{\mathrm{T}}, \tag{14}$$

$$\overrightarrow{E_y}(n) = [E_y(n), E_y(n-1), \cdots, E_y(n-k-2), E_y(n-k-1)]^{\mathrm{T}}. \tag{15}$$

Tap-coefficient column vectors $\overrightarrow{h_p}(n)$ are written as

$$\overrightarrow{h_p}(n) = \left[h_{p,0}(n), h_{p,1}(n), \cdots, h_{p,(k-2)}(n), h_{p,(k-1)}(n)\right]^{\mathrm{T}}. \tag{16}$$

Filter outputs are then given as

$$E_X(n) = \overrightarrow{h_{xx}}(n)^{\mathrm{T}}\overrightarrow{E_x}(n) + \overrightarrow{h_{xy}}(n)^{\mathrm{T}}\overrightarrow{E_y}(n), \tag{17}$$

$$E_Y(n) = \overrightarrow{h_{yx}}(n)^{\mathrm{T}}\overrightarrow{E_x}(n) + \overrightarrow{h_{yy}}(n)^{\mathrm{T}}\overrightarrow{E_y}(n). \tag{18}$$

The required number of taps k is determined from the impulse response of the transfer function of the link.

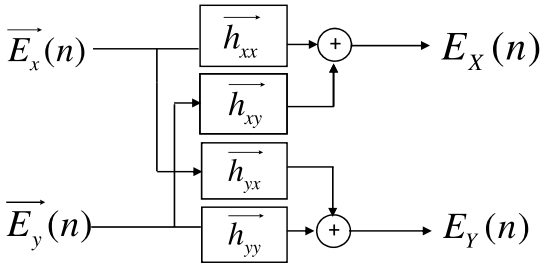


Fig. 4. Configuration of 2×2 butterfly-structured FIR filters.

© IEICE 2011
DOI: 10.1587/elex.8.1642
Received August 12, 2011
Accepted August 23, 2011
Published October 25, 2011

4.2 Filter-adaptation algorithms

Controlling the tap coefficients, we can generate the inverse transfer matrix of the link, which can not only compensate for linear impairments such as GVD and PMD but also demultiplex polarization tributaries by removing the fiber birefringence. When we compensate for fixed GVD of the link, we may use a fixed equalizer, where tap coefficients are predetermined, because the GVD value is not usually time-varying. Meanwhile, polarization-related impairments must be controlled in an adaptive manner. The fixed equalizer and the adaptive equalizer are usually concatenated.

Adaptive control of filter-tap coefficients of each FIR filter can be done by using the decision-directed least-mean-square (DD-LMS) algorithm as follows [24]:

$$\overrightarrow{h_{xx}}(n+1) = \overrightarrow{h_{xx}}(n) + \mu e_X(n)\overrightarrow{E_x}(n)^*, \tag{19}$$
$$\overrightarrow{h_{xy}}(n+1) = \overrightarrow{h_{xy}}(n) + \mu e_X(n)\overrightarrow{E_y}(n)^*, \tag{20}$$
$$e_X(n) = d_X(n) - E_X(n), \tag{21}$$
$$\overrightarrow{h_{yx}}(n+1) = \overrightarrow{h_{yx}}(n) + \mu e_Y(n)\overrightarrow{E_x}(n)^*, \tag{22}$$
$$\overrightarrow{h_{yy}}(n+1) = \overrightarrow{h_{yy}}(n) + \mu e_Y(n)\overrightarrow{E_y}(n)^*, \tag{23}$$
$$e_Y(n) = d_Y(n) - E_Y(n). \tag{24}$$

In these equations, μ is a step-size parameter, $e_{X,Y}(n)$ an error signal, and $d_{X,Y}(n)$ either a training symbol in the training mode or a decoded symbol in the tracking mode for each polarization tributary. After updating tap coefficients in the training mode so that the decoded symbol coincides with the desired symbol, we switch it into the tracking mode. In the case of $\times 2$ oversampling ($m = 2$), update of tap coefficients is done per every two samples.

When we cannot use the training sequence in the transmission system, we need to introduce an algorithm operating in the blind mode such as the DD-LMS algorithm without the training sequence and the constant-modulus algorithm (CMA) [25].

In CMA, error signals for updating tap coefficients are given instead of Eqs. (21) and (24) as

$$e_X(n) = (1 - |E_X(n)|^2)E_X(n), \tag{25}$$
$$e_Y(n) = (1 - |E_Y(n)|^2)E_Y(n). \tag{26}$$

This algorithm updates tap coefficients so that $|E_X(n)|^2$ and $|E_Y(n)|^2$ approach to unity. Since this algorithm does not require any feedback process, its computational complexity is lower than that of the DD-LMS.

In the case of M-ary PSK modulation formats, this algorithm works well because the signal has a constant envelope; however, the CMA-based equalization method is difficult to directly apply to M-ary QAM formats whose envelope has multi-levels. Another problem inherent in CMA is the singularity problem associated with polarization demultiplexing. When we use the CMA-based blind algorithm, it is likely that each output converges with the

© IEICE 2011
DOI: 10.1587/elex.8.1642
Received August 12, 2011
Accepted August 23, 2011
Published October 25, 2011

same polarization tributary [26]. Such improper polarization demultiplexing occurs especially when PDL cannot be ignored.

The DD-LMS algorithm with the training mode can avoid the singularity problem; however, it is sensitive to carrier phase fluctuations. To use long-tap FIR filters for signal equalization with the DD-LMS algorithm, we need to modify the FIR-filter structure so that it becomes insensitive to the carrier phase [27]. DSP circuits for equalizers should be implemented by considering the pros and cons of the two algorithms.

4.3 Clock-recovery function of the adaptive equalizer

A unique function of adaptive FIR filters is variable time delay with resolution much higher than the sampling time interval. If the number of filter taps is large enough, we can generate quasi-continuously-variable time delay for the received signal even by using discrete time-delay elements in the FIR filters. Owing to the quasi-continuously-variable time delay and the adaptive equalization algorithm, the signal waveform can be delayed so that the time best for symbol discrimination coincides with the sampling instant. In fact, this process is nothing but clock recovery.

So far, the clock recovery in the digital coherent receiver has been most commonly done in the following way [18]: First, data sampled by AD converters are up-sampled. Then, the clock is extracted from the up-sampled data through discrete Fourier transform (DFT). Next, by using the clock, the up-sampled data are re-sampled so as to keep one sample within one symbol interval. On the contrary, clock recovery simultaneously done with signal equalization is very attractive for implementation of DSP circuits [28].

In what follows, we analyze the property of sampling-phase adjustment with FIR filters. In the simulations, we assume that the clock frequency is locked between the transmitter and the receiver, as is usually the case in SONET/SDH networks, but that the initial sampling phase at AD conversion is uncontrolled.

Electric fields for x and y polarizations are independently modulated in the QPSK format, where each symbol is differentially encoded. The non-return-to-zero (NRZ) waveform includes 2^3 samples in one symbol duration. At the receiver, we assume $\times 2$ oversampling and the use of Nyquist filters having the roll-off parameter of 0.2 as anti-aliasing filters. The initial sampling instant is set to $(t = 0, T/2)$, $(t = T/8, 5T/8)$, $(t = T/4, 3T/4)$, or $(3T/8, 7T/8)$ within one symbol interval. The step-size parameter μ in the DD-LMS algorithm is 2^{-6}. The number of training symbols is 2^7, and the total number of symbols is 2^{14}.

Figure 5 shows bit-error rates calculated as a function of the energy per bit to noise spectral-power-density ratio, E_b/N_0, for four initial sampling phases mentioned above. Red and black curves show BERs of the x-polarization tributary and y-polarization tributary, respectively. Figures (a), (b), and (c) correspond to tap numbers of 1, 3, and 5, respectively. The one-tap FIR filter does not have any ability of giving time delay to the signal; therefore, BER curves are strongly dependent on the initial sampling phase. On the

© IEICE 2011
DOI: 10.1587/elex.8.1642
Received August 12, 2011
Accepted August 23, 2011
Published October 25, 2011

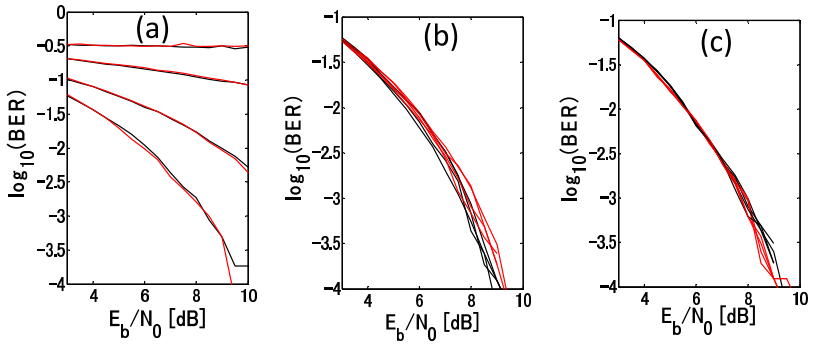


Fig. 5. Bit-error rates calculated as a function of E_b/N_0 for four initial sampling phases when we apply $\times 2$ oversampling. Numbers of taps are 1 in (a), 3 in (b), and 5 in (c). In all cases, the roll-off parameter of the Nyquist filter is 0.2. Red and black curves correspond to the x-polarization tributary and y-polarization tributary, respectively.

other hand, those for the three-tap and five-tap filters become insensitive to the initial sampling phase. We find that the FIR filter with five delay taps can entirely remove the dependence of BER on the initial sampling phase, achieving perfect clock recovery.

4.4 Frequency-domain adaptive equalization

Computational complexity of FIR filters scales with the number of delay taps; therefore, it becomes difficult to implement FIR filters having a large number of delay taps in ASICs or FPGAs due to large power consumption and high gate density. On the other hand, frequency-domain equalization (FDE) can reduce this computational cost by block-by-block signal processing and efficient implementation of discrete Fourier transform (DFT). The single-carrier FDE concept is shown in Fig. 6 [29]. After serial data of the received complex amplitude are divided into blocks with the serial-to-parallel converter, each block in the time domain is transformed into the frequency domain with DFT. Spectral components are then controlled by the frequency-domain equalizer. The block in the frequency domain is converted into the time domain with inverse DFT (IDFT).

The fully-adaptive FDE, which maintains all the advantages of the FIR-filter-based adaptive time-domain equalizer (TDE), has been proposed in [30]. Even in the block processing environment of FDE, it can work on the twofold-oversampled input sequence by introducing even and odd sub-equalizers, and

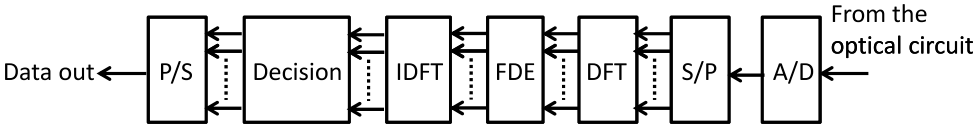


Fig. 6. Configuration of the single-carrier frequency-domain equalizer.

© IEICE 2011
DOI: 10.1587/elex.8.1642
Received August 12, 2011
Accepted August 23, 2011
Published October 25, 2011

we can achieve equalization, polarization demultiplexing, and clock recovery in the frequency domain. The interference between blocks due to GVD is usually managed by the overlap-save method.

To mitigate ISI due to GVD and to obtain high spectral efficiency in optical transmission systems, orthogonal frequency-domain multiplexing (OFDM) has been investigated as an alternative approach to single-carrier FDE mentioned above [31]. At the OFDM transmitter, IDFT of a block of data and succeeding parallel-to-serial conversion generate a multi-carrier signal as shown in Fig. 7 (a). At the receiver, after serial-to-parallel conversion, the received block is transformed into the frequency domain with DFT. Such a signal is then equalized, decoded, and converted to serial data as shown in Fig. 7 (b). Block interference due to GVD can be removed by cyclic prefix insertion, which is not shown in Fig. 7. In the OFDM system, we usually perform signal processing such as block synchronization, clock recovery, polarization demultiplexing, and phase estimation for multiple carriers, sending pilot symbols for reliable operation. Since blocks of data are prepared at the OFDM transmitter, it becomes easier to insert such pilot symbols than in the conventional scheme.

Further comparative study of these equalization methods is still needed to find the best solution to coherent optical communication systems.

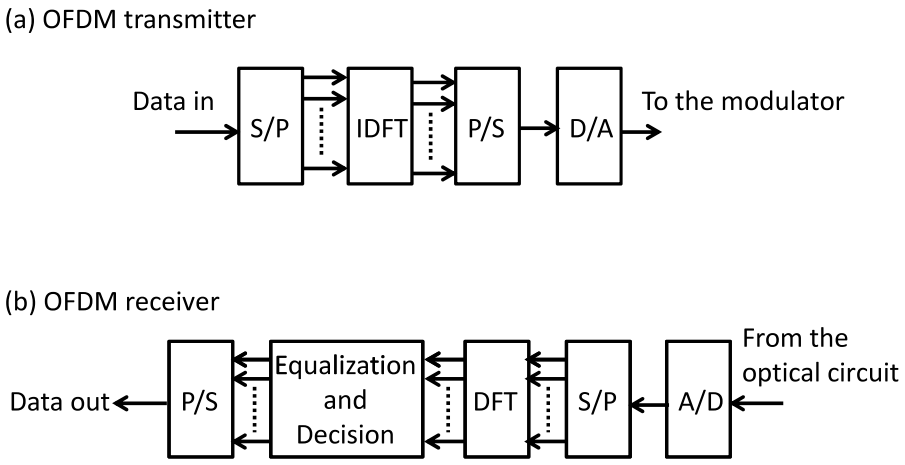


Fig. 7. Configurations of the OFDM transmitter (a) and the receiver (b).

5 Carrier-phase estimation

Since the linewidth of distributed feedback (DFB) semiconductor lasers used as the transmitter and LO typically ranges from 100 kHz to 10 MHz, the phase noise $\theta_n(t)$ varies much more slowly than the phase modulation $\theta_s(t)$. Therefore, by averaging the phase noise over many symbol intervals to improve the signal-to-noise ratio, it is possible to obtain an accurate phase estimate. Regarding Eq. (11) as the complex amplitude of the optical carrier itself, we sometimes call this phase-noise estimation process the carrier-phase estima-

© IEICE 2011
DOI: 10.1587/elex.8.1642
Received August 12, 2011
Accepted August 23, 2011
Published October 25, 2011

tion. In the following, assuming the M-ary PSK modulation, we explain the phase estimation procedure [6, 7, 8].

The phase of the complex amplitude obtained from Eq. (11) contains both the phase modulation $\theta_s(i)$ and the phase noise $\theta_n(i)$, where i represents the sample number. The procedure to estimate θ_n is shown in Fig. 8, where the case of QPSK is shown for simplicity. We take the Mth power of the measured complex amplitude $E(i)$, because the phase modulation is removed from $E(i)^M$ in the case of the M-ary PSK modulation format. Subtracting the phase noise thus estimated from the measured phase, we can restore the phase modulation. This is a feedfoward algorithm, which is suitable for DSP implementation. However, note that this algorithm cannot directly be applied to high-order QAM formats. For example, in the case of 16 QAM, we need to discriminate the level of each symbol and apply the 4th power algorithm to the outer four constellation points and the inner four constellation points separately.

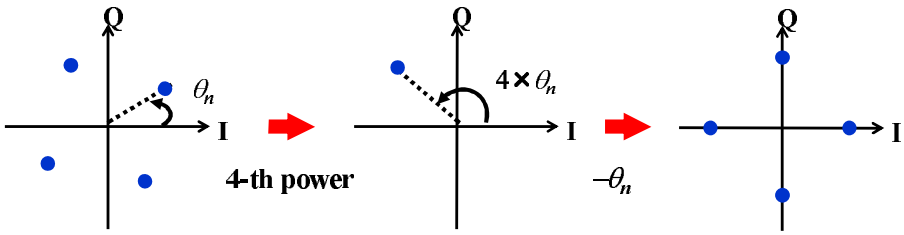


Fig. 8. Principle of the Mth-power phase estimation method. For simplicity, the case of QPSK ($M = 4$) is shown. Taking the Mth power of the received complex amplitude, we can eliminate the phase modulation and measure the phase noise.

In actual phase estimation, we average $E(i)^M$ over $2k+1$ samples to improve the signal-to-noise ratio of the estimated phase reference. The estimated phase is thus given as

$$\theta_e(i) = \arg\left(\sum_{j=-k}^{k} E(i+j)^M\right)/M. \tag{27}$$

The phase modulation $\theta_s(i)$ is determined by subtracting $\theta_e(i)$ from the measured phase of $\theta(i)$. The phase modulation is then discriminated among M symbols. Figure 9 shows the DPS circuit for such phase estimation. The optimum averaging span is dependent on the laser linewidth. When the linewidth is narrower, the optimum averaging span is longer, which gives us the better BER performance.

The symbols thus obtained have the phase ambiguity by $2\pi/M$. To cope with such phase ambiguity, the data should be differentially encoded at the transmitter. In such a case, differentially decoding the discriminated symbol, we can solve the phase ambiguity problem, although the bit-error rate is doubled by error multiplication.

© IEICE 2011
DOI: 10.1587/elex.8.1642
Received August 12, 2011
Accepted August 23, 2011
Published October 25, 2011

Figure 10 shows simulation results of BER characteristics of 10-Gsymbol/s QPSK signals, where the laser linewidth is varied [32]. We assume that linewidths of lasers for the transmitter laser and LO are the same. The averaging span is optimized dependently on the linewidth to have the best BER characteristics. The power penalty at BER=10^{-4} is less than 2 dB when the laser linewidth is as large as 5 MHz.

We can also use a one-tap FIR filter adapted by the LMS algorithm to estimate the phase noise [9]. Such a scheme can be applied directly to QAM formats; however, its computational complexity is higher than that of the feedforwad phase estimation, because the LMS algorithm includes the feedback process. We should judge which scheme is better, considering the DSP implementation issue of the algorithms as well as their performances.

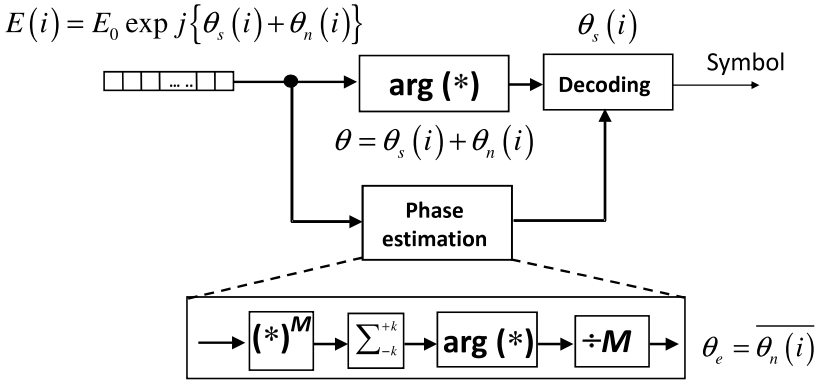


Fig. 9. DSP circuit for M-th power phase estimation.

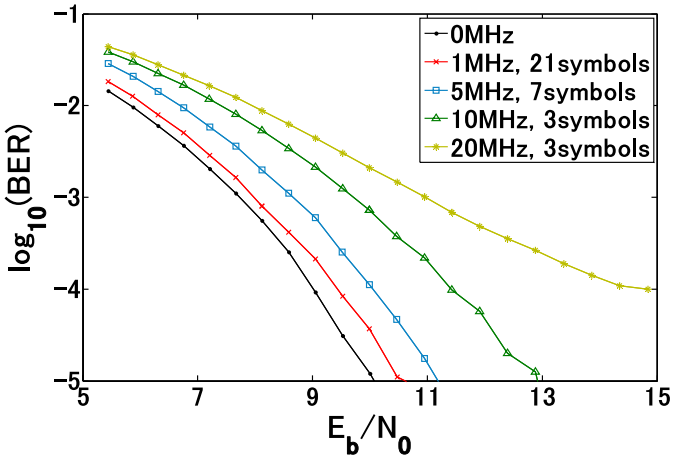


Fig. 10. Simulation results of BER characteristics of 10-Gsymbol/s QPSK signals, where the laser linewidth is changed. The averaging span shown in the inset is optimized to have the best BER characteristics.

© IEICE 2011
DOI: 10.1587/elex.8.1642
Received August 12, 2011
Accepted August 23, 2011
Published October 25, 2011

6 Transmission characteristics of multi-level modulated signals

High-order optical QAM formats, such as 16, 64, and 256 QAM, have attracted significant attention because of their spectrally-efficient transmission characteristics in dense WDM as well as POLMUX environments [33, 34, 35]. The recent development of digital coherent optical receivers may enable the use of such sophisticated modulation formats in the near future.

Although the spectral efficiency can potentially be improved with higher-order QAM formats such as 16 QAM, 64 QAM, and 256 QAM, their transmission characteristics may suffer more seriously from nonlinear impairments due to self-phase modulation (SPM) and cross-phase modulation (XPM) than that of 4 QAM (QPSK). This section aims at analyzing the performance of WDM POLMUX high-order QAM transmission through intensive computer simulations [36, 37]. The model of the transmission system is as follows: The dispersion-unmanaged link has 80-km-long single-mode-fiber (SMF) spans. We assume large-core SMFs, which have the GVD value D of 19 ps/nm/km ($\beta_2 = -24\,\mathrm{ps}^2/\mathrm{km}$), the nonlinearity coefficient γ of 1.1 /W/km, and the loss coefficient α of 0.17 dB/km at the wavelength of 1550 nm. We use the 50% return-to-zero (RZ) waveform for the envelope of the complex amplitude of the signal electric field. Differentially-encoded optical QAM signals are filtered out by root Nyquist filters with the roll-off parameter of 0.3 before transmission. An erbium-doped fiber amplifier (EDFA) with the noise figure of 4 dB compensates for the loss of each span. Linewidths of transmitter lasers are assumed to be negligible in our calculations to investigate only the nonlinear effect. The WDM channel spacing is twice as large as the symbol rate, and the maximum number of WDM channels is five.

We calculate QAM transmission characteristics of a single channel, co-polarized three WDM channels, co-polarized five WDM channels, and POLMUX five WDM channels, where the symbol rate is 12.5 Gsymbol/s and the WDM channel spacing 25 GHz. We select the center WDM channel for BER estimation, which is most seriously affected by XPM between WDM channels. In the case of POLMUX transmission, we evaluate BERs of one of the two polarization tributaries. The number of spans n for each QAM format is determined such that the BER of the polarization tributary of the center WDM channels becomes lower than 10^{-3} at the optimum launched power, when POLMUX five WDM channels are transmitted.

Figures 11 (a)-(d) show BERs of 4 QAM, 16 QAM, 64 QAM, and 256 QAM signals, respectively, calculated as a function of the launched average power P_{ave}. Powers of all channels are changed simultaneously. Green, red, black, and blue curves represent BERs when we transmit a single channel, co-polarized three WDM channels, co-polarized five WDM channels, and POLMUX five WDM channels, respectively. Numbers of spans n corresponding to Figs. (a)-(d) are 160, 37, 10, and 3, respectively, resulting in total transmission distances of 12,800 km, 2,960 km, 800 km, and 240 km. Note that above the optimum power about -9 dBm ~ -8 dBm, the BER

© IEICE 2011
DOI: 10.1587/elex.8.1642
Received August 12, 2011
Accepted August 23, 2011
Published October 25, 2011

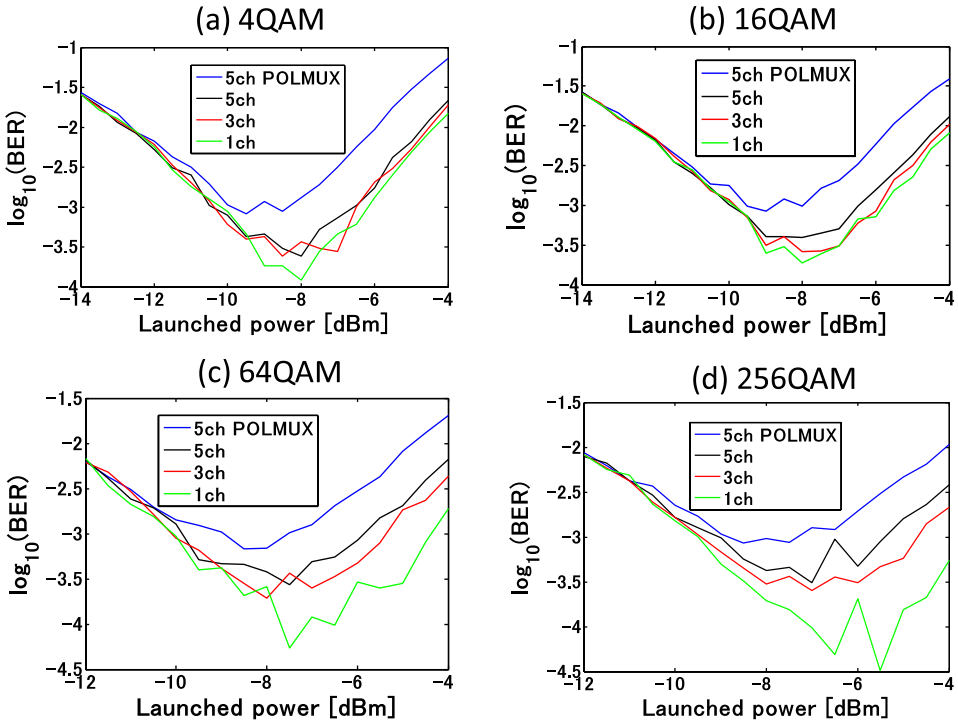


Fig. 11. BER characteristics of QAM transmission systems. (a): 4 QAM, (b): 16 QAM, (c): 64 QAM, and (d): 256 QAM. Green, red, black, and blue curves represent BERs when we transmit a single channel, co-polarized three WDM channels, co-polarized five WDM channels, and POLMUX five WDM channels, respectively. The symbol rate is 12.5 Gsymbol/s, and the WDM channel spacing is 25 GHz. Numbers of spans n corresponding to (a)-(d) are 160, 37, 10, and 3, respectively.

performance is degraded by nonlinear impairments stemming from SPM and XPM between WDM channels and POLMUX channels.

Dots in Fig. 12 show the maximum number of spans n as a function of the order of QAM m, when POLMUX five WDM channels are transmitted. We find that n is inversely proportional to m as seen from the solid line and that transmission distances of 64 QAM and 256 QAM systems are severely limited below 1,000 km. Thus, when we aim at higher spectral efficiency with higher-order QAM, the performance of such system will strongly be restricted by fiber nonlinearity. Although the back-propagation method was proposed to compensate for fiber nonlinearity [38, 39], huge computational complexity prevents its practical application. Finding practical countermeasure against fiber nonlinearity is one of the most crucial issues in coherent optical communication systems.

7 Future prospects

The progress of digital coherent technologies is very rapid. However, the following is the technical problems that must be tackled and accomplished

© IEICE 2011
DOI: 10.1587/elex.8.1642
Received August 12, 2011
Accepted August 23, 2011
Published October 25, 2011

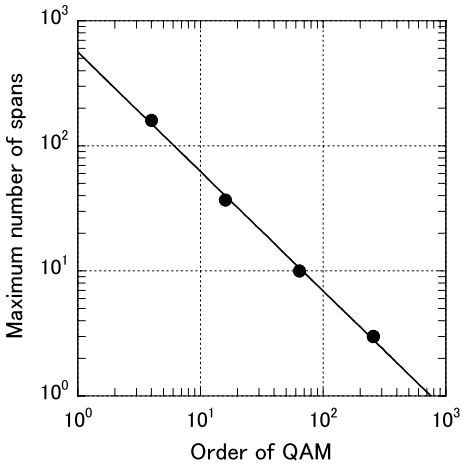


Fig. 12. Maximum number of spans n as a function of the order of QAM m. The solid line shows the relation of $n \propto m^{-1}$.

before the practical coherent optical communication system is realized in the near future.

[1] Hybrid/monolithic integration of phase and polarization diversities, double-balanced photodiodes, and a local oscillator is an important technical task, which enables cost reduction of the coherent receiver and improves system stability.

[2] A tunable local oscillator with a narrow linewidth is still the key component of the high-performance coherent receiver.

[3] High-speed operation of the coherent receiver relies on the development of high-speed ADC and DSP. The processing speed higher than 50 GSample/s is desirable for >100-Gbit/s applications. Parallelization techniques in the time domain or the frequency domain at the optical stage may solve the difficulty in increasing the sampling rate of ADC.

[4] More flexible signal processing should be available in the DSP core. Development of algorithms having lower computational complexity is also indispensable. Generally, insertion of training/pilot symbols may help to improve stability and flexibility of signal processing compared to the blind-mode processing. We should examine applicability of insertion of training/pilot symbols in practical optical communication systems.

[5] For long-distance transmission of multi-level modulated optical signals, fiber nonlinearity ultimately limits the system performance. It is an crucial consideration to develop efficient algorithms for fiber nonlinearity compensation.

8 Conclusions

After describing the history of the coherent optical communication system, we have shown how digital signal processing is playing an important role in

© IEICE 2011
DOI: 10.1587/elex.8.1642
Received August 12, 2011
Accepted August 23, 2011
Published October 25, 2011

the new-generation coherent receiver, called the digital coherent receiver. A great variety of digital signal processing can enhance the system performance; however, we still need to develop DSP algorithms for stable operation of the total receiving system, and low computational complexity of them is an crucial consideration. From the viewpoint of optical devices, device integration is one of the most important technical problems because the digital coherent receiver has a more complex configuration than the IMDD receiver.

The digital coherent receiver enables the use of multi-level modulation formats, which might improve the spectral efficiency; however, fully to enjoy the advantage of such modulation formats, we have to cope with nonlinear impairments of the transmission system. It is still an open question how to mitigate nonlinear impairments with DSP.

The combination of coherent detection and DSP provides us with new capabilities that were not possible without detection of the phase of the optical signal. Tackling the remaining problems, we are going to innovate optical communication systems with the born-again coherent optical technology.

Acknowledgments

The author thanks K. Igarashi, Md. S. Faruk, Y. Mori, and C. Zhang of The University of Tokyo for fruitful discussions. This work was supported in part by Strategic Information and Communications R&D Promotion Programme (SCOPE) (081503001), the Ministry of Internal Affairs and Communications, Japan, and Grant-in-Aid for Scientific Research (A) (22246046), the Ministry of Education, Science, Sports and Culture, Japan.



Kazuro Kikuchi
was born in Miyagi Prefecture, Japan, on March 6, 1952. He received the B.S. degree in electrical engineering and the M.S. and Ph.D. degrees in electronic engineering from the University of Tokyo, Tokyo, Japan, in 1974, 1976, and 1979, respectively. In 1979, he joined Department of Electronic Engineering at the University of Tokyo. After working at Research Center for Advanced Science and Technology (RCAST) (1997-2008) and Department of Frontier Informatics (2008-2009), he has been a professor at Department of Electrical Engineering and Information Systems since 2009. From April 1986 to March 1987, he was on leave of absence from the University of Tokyo with Bell Communications Research (Bellcore), NJ, USA. He has been a board member of Alnair Labs Corporation since 2002.
Since 1979, his work has been on the optical communication system. He is currently involved in coherent optical communication systems that realize multi-level modulation formats with digital signal processing.
Dr. Kikuchi is a Member of the IEEE Photonics Society, a Member of the Optical Society (OSA), and a Fellow of the Institute of Electronics, Information and Communication Engineers (IEICE).

© IEICE 2011
DOI: 10.1587/elex.8.1642
Received August 12, 2011
Accepted August 23, 2011
Published October 25, 2011